Inorganic Chemistry
Article

Inorg. Chem. **2010**, *49*, 3029–3034 **3029**
DOI: 10.1021/ic9025848

Rhodium−Germanium Carbonyl Complexes

Richard D. Adams* and Eszter Trufan

Department of Chemistry and Biochemistry, University of South Carolina, Columbia, South Carolina 29208

Received December 28, 2009

The compound $Rh(CO)_4GePh_3$, **3**, was obtained in a high yield (95%) from the reaction of $[Rh(CO)_2Cl]_2$ with $LiGePh_3$ under a CO atmosphere. Reaction of **3** with $HGePh_3$ yielded the new dirhodium compound $Rh_2(CO)_6(GePh_3)_2(\mu\text{-}GePh_2)$, **4** (55% yield), by a loss of CO and the combination of one equivalent of $HGePh_3$ with two equivalents of **3**. Compound **4** contains contains a Rh−Rh bond and a bridging $GePh_2$ ligand formed by cleavage of a phenyl group from a $GePh_3$ ligand. Compound **4** reacts with $Pt(PBu^t_3)_2$ to add a $Pt(PBu^t_3)$ to the Rh−Rh bond to form the compound $PtRh_2(CO)_6(GePh_3)_2(PBu^t_3)(\mu\text{-}GePh_2)$, **5** (42% yield). Fenske−Hall molecular orbitals were calculated for compounds **4** and **5** to explain the nature of the metal−metal bonding in these compounds. Compounds **3**−**5** were fully characterized by IR, NMR, and single-crystal X-ray diffraction analyses.

Introduction

Rhodium carbonyl species are important intermediates in a variety of homogeneous catalytic reactions including hydrogenation,[1] hydroformylation,[2] hydrosilylation,[3] and silylformylation reactions,[4] and in the famous acetic acid synthesis involving the carbonylation of methanol.[5] Germanium has been shown to be a valuable modifier of rhodium for the selective catalytic hydrogenation of citral and other unsaturated hydrocarbons.[6−8]

Although the first rhodium−germanium complexes were synthesized over 40 years ago,[9] there has been only a smattering of new Rh−Ge complexes reported since that initial report.[10−12] We have recently obtained the first polynuclear rhodium−germanium carbonyl cluster complexes $Rh_3(CO)_5(GePh_3)(\mu\text{-}GePh_2)_3(\mu_3\text{-}GePh)(\mu\text{-}H)$, **1**, and $Rh_8(CO)_{12}(\mu_4\text{-}GePh)_6$, **2**, from the reaction of $Rh_4(CO)_{12}$ with Ph_3GeH, eq 1.[12]

$$Rh_4(CO)_{12} \xrightarrow[97\ ^oC]{+HGePh_3} \quad (1)$$

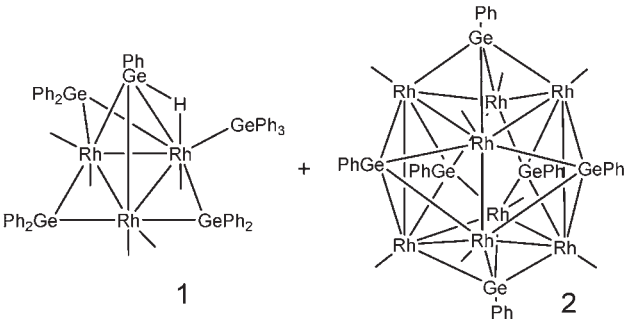

Compound **1** contains a terminal triphenylgermyl ligand, a triply bridging phenylgermylyne ligand, and three edge-bridging diphenylgermylene ligands all in the same trirhodium complex. Compound **2** contains four quadruply bridging phenylgermylyne ligands. The germylene and germylyne ligands were formed by the cleavage of phenyl groups from the germanium atom of the $HGePh_3$ reagent.

Curiously, after all these years, no one has yet isolated and structurally characterized a rhodium complex of the general formulation, $R_3ERh(CO)_4$, where R = any alkyl or aryl substituent and E = any group 14 element, a key intermediate species in certain catalytic reactions.[13] Herein, we report the

*To whom correspondence should be addressed. E-mail: Adams@mail.chem.sc.edu.

(1) James, B. R. *Homogeneous Hydrogenation*; Wiley: New York, 1973; pp 262−286.
(2) (a) Masters, C. *Homogeneous Transition Metal Catalysis - A Gental Art*; Chapman and Hall: London, 1981; pp 120−135. (b) Liu, G.; Garland, M. *J. Organomet. Chem.* **2000**, *608*, 76–85.
(3) Ojima, I.; Clos, N.; Donovan, R. J.; Ingallina, P. *Organometallics* **1990**, *9*, 3127–3133.
(4) Ojima, I.; Ingallina, P.; Donovan, R. J.; Clos, N. *Organometallics* **1991**, *10*, 38–41.
(5) Forster, D.; Dekleva, T. W. *J. Chem. Educ.* **1986**, *3*, 204–206.
(6) Ekou, T.; Vicente, A.; Lafaye, G.; Especel, C.; Marecot, P. *Appl Catal. A Gen.* **2006**, *314*, 73–80.
(7) Lafaye, G.; Micheaud-Especel, C.; Montassier, C.; Marecot, P. *Appl. Catal. A Gen.* **2002**, *230*, 19–30.
(8) Lafaye, G.; Micheaud-Especel, C.; Montassier, C.; Marecot, P. *Appl. Catal. A Gen.* **2004**, *257*, 107–117.
(9) Glockling, F.; Hill, G. C. *J. Organomet. Chem.* **1970**, *22*, C48–C50.
(10) Veith, M.; Mueller, A.; Stahl, L.; Noetzel, M.; Jarczyk, M.; Huch, V. *Inorg. Chem.* **1996**, *35*, 3848–3855.
(11) Dysard, J. M.; Tilley, T. D. *Organometallics* **2000**, *19*, 2671–2675.
(12) Adams, R. D.; Captain, B.; Smith, J. L., Jr. *Inorg. Chem.* **2005**, *44*, 4276–4281.
(13) Li, C.; Widjaja, E.; Chew, W.; Garland, M. *Angew. Chem., Int. Ed.* **2002**, *41*, 3786–3789.

Published on Web 02/11/2010

synthesis and structural characterization of the complex $Ph_3GeRh(CO)_4$, a reasonable model for all $RRh(CO)_4$ species, and a study of its reaction with $HGePh_3$.

Experimental Section

General Data. All reactions were performed under a nitrogen atmosphere unless otherwise specified. Reagent grade solvents were dried according to standard procedures and were freshly distilled prior to use. Infrared spectra were recorded on a Thermo-Nicolet Avatar 360 FT-IR spectrophotometer. ^1H NMR spectra were recorded on a Mercury 300 spectrometer operating at 300.1 MHz. $^{31}P\{^1H\}$ NMR spectra were recorded on a Varian Mercury 400 spectrometer operating at 161.9 MHz and were externally referenced against 85% *ortho*-H_3PO_4. Mass spectrometric (MS) measurements performed by a direct-exposure probe using electron impact ionization (EI) were made on a VG 70S instrument. Product separations were performed by TLC in the air on Analtech 0.5 mm silica gel 60 Å F_{254} glass plates. $Rh_2(CO)_4(\mu\text{-}Cl)_2$ was purchased from Strem Chemicals, Inc. $HGePh_3$ was purchased from Aldrich and was used without further purification.

Synthesis of $Rh(CO)_4GePh_3$, 3. A total of 31.4 mg (0.103 mmol) of $HGePh_3$ was dissolved 20 mL of hexane in a 100 mL three-neck flask. To this solution was added 0.067 mL of a 1.6 M BuLi solution in hexane. After 5 min of stirring at room temperature, the solution was placed under a CO atmosphere, and 20.1 mg (0.052 mmol) of $[Rh(CO)_2Cl]_2$ was added and stirred for 45 min. The IR spectrum of the solution showed only three absorptions subsequently assigned to $Rh(CO)_4GePh_3$. The solution was filtered under CO, and crystals were grown by slow evaporation of the solvent under a slow and continuous purge of CO. The crystalline product that formed upon evaporation of the solvent was pure $Rh(CO)_4GePh_3$, **3**, 51.7 mg (95% yield). Spectral data for **3**: IR ν_{CO} (cm^{-1} in hexane): 2102 (s), 2049(m), 2025 (vs). ^1H NMR ($CDCl_3$, in ppm): δ 7.31−7.51 (m, 15 H, Ph).

Synthesis of $Rh_2(CO)_6(\mu\text{-}GePh_2)(GePh_3)_2$, 4. A total of 51.7 mg (0.099 mmol) of $Rh(CO)_4GePh_3$ was dissolved 20 mL of hexane in a 100 mL three-neck flask under a CO atmosphere. To this solution was added 15.3 mg (0.050 mmol) of $HGePh_3$, and this was stirred for 15 min. The solvent was removed in vacuo. The residue was dissolved in a minimum amount of CH_2Cl_2 and was transferred into a Schlenk tube. A small amount of hexane was added, and the tube was purged with CO, sealed, and cooled to −80 °C. A total of 32.9 mg of yellow crystals of $Rh_2(CO)_6(\mu\text{-}GePh_2)(GePh_3)_2$, **4** (55% yield), formed. Spectral data for **4**: IR ν_{CO} (cm^{-1} in hexane): 2094 (w), 2052(m), 2030 (vs). ^1H NMR ($CDCl_3$, in ppm): δ 7.06−7.67 (m, 30 H, Ph).

Synthesis of $PtRh_2(CO)_6(\mu\text{-}GePh_2)(GePh_3)_2(PBu^t_3)$, 5. A total of 29.3 mg (0.024 mmol) of $Rh_2(CO)_6(GePh_2)(GePh_3)_2$ was dissolved in 5 mL of CH_2Cl_2 in a 10 mL Schlenk tube. To this solution was added a 14.5 mg amount of $Pt(PBu^t_3)_2$, which was stirred for 10 min at room temperature. The solvent was removed in vacuo, and the residue was transferred to TLC plates in a minimum amount of CH_2Cl_2 and was separated in air by using a 4:1 hexane−methylene chloride elution solvent mixture to yield an orange band that gave 16.5 mg of $PtRh_2(CO)_6(\mu\text{-}GePh_2)(GePh_3)_2(PBu^t_3)$, **5** (42% yield). Spectral data for **5**: IR ν_{CO} (cm^{-1} in hexane): 2079 (w), 2045 (w), 2018(s), 1870(w), 1824 (m). ^1H NMR ($CDCl_3$, in ppm): δ 7.02−7.62 (m, 40 H, Ph), 1.33 (d, 9H, CH_3, $^1J_{H-H}$ = 13.1 Hz). $^{31}P\{^1H\}$ NMR ($CDCl_3$, in ppm) at 25 °C: δ 107.16 (t, 1P, $^1J_{^{195}Pt-^{31}P}$ = 4993 Hz, $^2J_{^{103}Rh-^{31}P}$ = 8.1 Hz). Mass Spec. (EI): a weak parent ion was observed at m/z = 1606. The isotope pattern is consistent with the presence of one platinum and three germanium atoms.

Crystallographic Analyses. Colorless crystals of **3** were grown by slow evaporation of the solvent from the reaction mixture under a slow stream of CO. Yellow crystals of **4** were grown in a flask from a hexane solution under a CO atmosphere at −79 °C, and red crystals of **5** were grown from a solution in a CH_2Cl_2/hexane solvent mixture at room temperature. X-ray intensity data were measured by using a Bruker SMART APEX CCD-based diffractometer by using Mo Kα radiation (λ = 0.71073 Å). The raw data frames were integrated with the SAINT+ program by using a narrow-frame integration algorithm.[14] Corrections for Lorentz and polarization effects were also applied with SAINT+. An empirical absorption correction based on the multiple measurement of equivalent reflections was applied using the program SADABS. All structures were solved by a combination of direct methods and difference Fourier syntheses and refined by full-matrix least-squares on F^2 using the SHELXTL software package.[15] All non-hydrogen atoms were refined with anisotropic displacement parameters. All hydrogen atoms were placed in geometrically idealized positions and included as standard riding atoms during the least-squares refinements. Crystal data, data collection parameters, and results of the analyses are listed in Table 1. All compounds crystallized in the triclinic crystal system. The space group $P\bar{1}$ was assumed and confirmed by the successful refinement and solution of the structure in each case. The asymmetric crystal unit of **3** and **5** contains one independent formula equivalent of the complex, while **4** with Z = 4 contains two formula equivalents of the cluster in its asymmetric crystal unit.

Table 1. Crystallographic Data for Compounds **3**, **4**, and **5**

compound	**3**	**4**	**5**
empirical formula	$RhGeO_4C_{22}H_{15}$	$Rh_2Ge_3O_6C_{54}H_{40}$	$PtRh_2Ge_3PO_6C_{66}H_{67}$
fw	518.84	1208.45	1605.85
cryst syst	triclinic	triclinic	triclinic
lattice parameters			
a (Å)	10.0145(7)	14.2850(7)	13.9155(8)
b (Å)	10.5419(7)	19.4277(9)	14.3362(8)
c (Å)	11.0141(8)	21.1061(10)	17.191(1)
α (deg)	86.833(1)	63.872(1)	73.172(1)
β (deg)	68.871(1)	74.312(1)	75.041(1)
γ (deg)	82.025(1)	68.765(1)	80.862(1)
V (Å^3)	1074.10(13)	4858.6(4)	3158.3(3)
space group	$P\bar{1}$ (#2)	$P\bar{1}$ (#2)	$P\bar{1}$ (#2)
Z value	2	4	2
ρ_{calc} (g/cm^3)	1.604	1.652	1.689
μ (Mo K$_\alpha$) (mm^{-1})	2.190	2.549	4.200
temperature (K)	150(2)	150(2)	294(2)
$2\Theta_{max}$ (deg)	52.84	56.64	52.74
no. obs. ($I > 2\sigma(I)$)	5372	24155	12878
no. params	313	1171	721
goodness of fit GOF[a]	0.990	0.979	1.056
max. shift in cycle	0.001	0.180	0.017
residuals: R1, wR2[a]	0.0332, 0.0745	0.0532, 0.0854	0.0745, 0.1582
absorption correction, max/min	SADABS 1.000/0.815	SADABS 1.000/0.807	SADABS 1.000/0.463
largest peak in final diff. map (e$^-$/Å^3)	0.538	0.874	2.763

[a] $R = \sum_{hkl}(||F_{obs}| - |F_{calc}||)/\sum_{hkl}|F_{obs}|$; $R_w = [\sum_{hkl}w(|F_{obs}| - |F_{calc}|)^2/\sum_{hkl}wF_{obs^2}]^{1/2}$; $w = 1/\sigma^2(F_{obs})$; GOF = $[\sum_{hkl}w(|F_{obs}| - |F_{calc}|)^2/(n_{data} - n_{vari})]^{1/2}$.

Molecular Orbital Calculations. All molecular orbital calculations reported herein were performed by using the Fenske−Hall method.[16] The calculations were performed utilizing a

(14) *SAINT+*, version 6.2a; Bruker Analytical X-ray Systems, Inc.: Madison, WI, 2001.

(15) Sheldrick, G. M. *SHELXTL*, version 6.1; Bruker Analytical X-ray Systems, Inc.: Madison, WI, 1997.

(16) (a) Hall, M. B.; Fenske, R. F. *Inorg. Chem.* **1972**, *11*, 768–775. (b) Webster, C. E.; Hall, M. B. In *Theory and Applications of Computational Chemistry: The First Forty Years*; Dykstra, C., Ed.; Elsevier: Amsterdam, 2005; Ch. 40, pp 1143−1165.

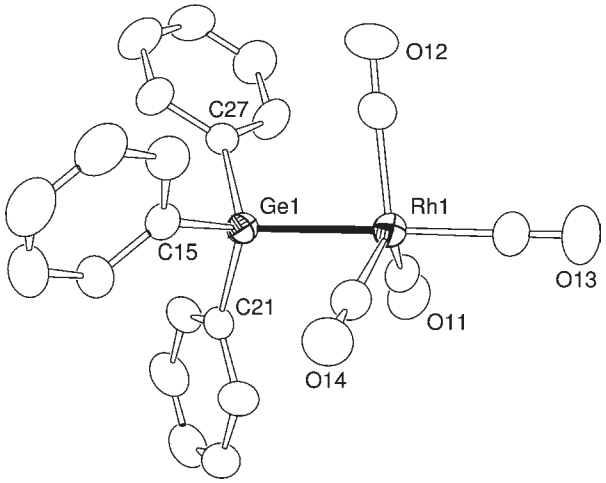

Figure 1. An ORTEP diagram of the molecular structure of $Rh(CO)_4(GePh_3)$, **3**, showing 30% thermal ellipsoid probability. Selected bond distances (Å) and angles (deg) are as follows: Rh(1)−Ge(1) = 2.5061(4), Rh(1)−C(14) = 1.943(3), Rh(1)−C(12) = 1.947(3), Rh(1)−C(11) = 1.949(3), Rh(1)−C(13) = 1.977(4); C(13)−Rh(1)−Ge(1) = 179.01(10), C(14)−Rh(1)−Ge(1) = 83.61(10), C(12)−Rh(1)−Ge(1) = 84.67(9), C(11)−Rh(1)−Ge(1) = 84.21(9), C(14)−Rh(1)−C(13) = 96.26(14), C(12)−Rh(1)−C(13) = 96.25(14), C(11)−Rh(1)−C(13) = 95.04(14).

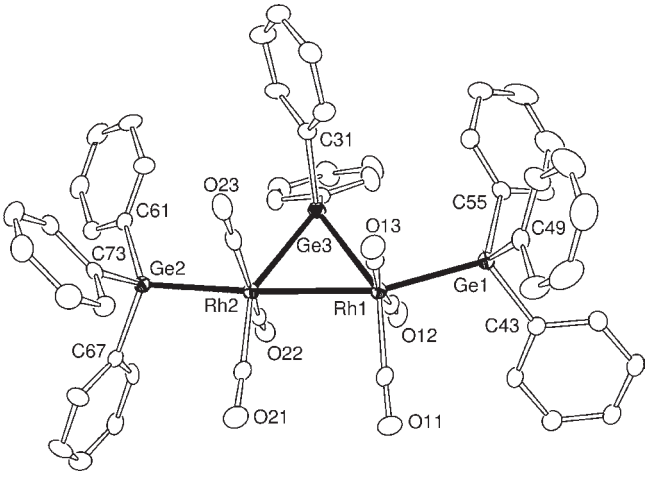

Figure 2. An ORTEP diagram of the molecular structure of $Rh_2(CO)_6(GePh_3)_2(\mu\text{-}GePh_2)$, **4**, showing 30% thermal ellipsoid probability. Selected bond distances (Å) and angles (deg) are as follows. Molecule **1**: Rh(1)−Rh(2) = 2.8766(6), Rh(1)−Ge(1) = 2.4961(7), Rh(1)−Ge(3) = 2.4728(6), Rh(2)−Ge(2) = 2.5059(6), Rh(2)−Ge(3) = 2.4815(7); Rh(1)−Ge(3)−Rh(2) = 70.990(19), 70.830(19), Rh(1)−Rh(2)−Ge(3) = 54.363(16), Rh(2)−Rh(1)−Ge(3) = 164.62(2), Rh(1)−Rh(2)−Ge(2) = 174.16(2). Molecule **2**: Rh(3)−Rh(4) = 2.8716(6), Rh(3)−Ge(4) = 2.5000(7), Rh(3)−Ge(6) = 2.4706(6), Rh(4)−Ge(5) = 2.4821(7), Rh(4)−Ge(6) = 2.4847(7); Rh(4)−Rh(3)−Ge(6) = 54.815(16), Rh(3)−Ge(6)−Rh(4) = 70.830(19), Rh(4)−Rh(3)−Ge(4) = 168.73(2), Rh(3)−Rh(4)−Ge(5) = 174.41(2).

graphical user interface developed[17] to build inputs and view outputs from stand-alone Fenske−Hall and MOPLOT2 binary executables.[18] Contracted double-ζ basis sets were used for the Rh 4d, Pt 5d, Ge 4p, P 3p, and C and O 2p atomic orbitals. The Fenske−Hall scheme is a nonempirical approximate method that is capable of calculating molecular orbitals for very large transition metal systems. For these calculations, the input structures were obtained from the positional parameters from the crystal structure analyses. The structures were not optimized in these calculations. The t-butyl groups on the phosphine ligands and the phenyl groups on the $GePh_3$ and $GePh_2$ ligands were replaced by hydrogen atoms to give PH_3, GeH_3, and GeH_2 ligands in the model.

Results and Discussion

The compound $Rh(CO)_4GePh_3$, **3**, was obtained in a high yield (95%) from the reaction of $[Rh(CO)_2Cl]_2$ with $LiGePh_3$ under a CO atmosphere for 45 min. Compound **3** is unstable in solution in the absence of a CO atmosphere, but crystals survive long enough in air so that one could be quickly transferred to a goniometer head at room temperature. A high quality single-crystal X-ray diffraction data set was obtained by rapidly cooling to −123 °C. An ORTEP diagram of the molecular structure of **3** is shown in Figure 1. The rhodium atom in **3** contains a trigonal bipyramidal arrangement of four CO ligands and one $GePh_3$ ligand. The $GePh_3$ ligand occupies one of the axial sites. The Rh−Ge distance of 2.5061(4) Å is slightly shorter than the Rh−Ge distance, 2.533(3) Å, to the $GePh_3$ ligand in the complex $Rh_3(CO)_5(GePh_3)(\mu\text{-}GePh_2)_3(\mu_3\text{-}GePh)(\mu\text{-}H)$, **1**.[12] The Rh−C distances to the CO ligands in the equatorial plane are very similar, 1.943(3), 1.947(3), 1.949(3) Å, and significantly shorter than the Rh−C distance to the CO ligand, 1.977(4) Å, in the position trans to the Ge atom. Interestingly, the C−Rh−C angles between the axial CO ligand and the equatorial CO ligands in **1** are larger, 96.26(14)°, 96.25(14)°, and 95.04(14)°, than the Ge−Rh−C, 83.61(10)°; C(12)−Rh(1)−Ge(1), 84.67(9) °; and C(11)−Rh(1)−Ge(1), 84.21(9)° angles. Examination shows that the three phenyl rings on the $GePh_3$ ligand have adopted a staggered conformation with respect to the equatorial CO ligands on the rhodium atom which in turn allows the CO ligands to move toward the $GePh_3$ ligand. The IR spectrum of **3** in the CO stretching regions exhibits three absorptions at 2102 (s), 2049(m), and 2025 (vs), which is consistent with the axially substituted C_{3v} structure found in the solid state and indicates that the structure is the same in solution and there are no additional isomers present.[13]

When compound **3** was treated with one-half of an equivalent of $HGePh_3$ under a CO atmosphere at room temperature for 15 min, the new dirhodium complex $Rh_2(CO)_6(\mu\text{-}GePh_2)(GePh_3)_2$, **4**, was obtained in 55% yield. Compound **4** was characterized by IR, ^1H NMR, and a single crystal X-ray diffraction analysis. There are two independent molecules in the asymmetric crystal unit of **4**. Both molecules are structurally similar. An ORTEP diagram of the molecular structure of one of these two molecules of **4** is shown in Figure 2. The complex contains two $Rh(CO)_3(GePh_3)$ groups that are joined by a Rh−Rh single bond that is bridged by a $GePh_2$ ligand. The Rh−Rh bond, 2.8766(6) Å for molecule **1** (2.8716(6) Å for molecule **2**), is slightly longer than the unbridged Rh−Rh bond distance, 2.827(1) Å, found in the compound $Rh_2(CO)_6[P(cyclo\text{-}C_5H_9)_3]_2$,[19] but within the range of the $GePh_2$ bridged Rh−Rh bond distances reported for $Rh_3(CO)_5(GePh_3)(\mu\text{-}GePh_2)_3(\mu_3\text{-}GePh)(\mu\text{-}H)$, **1** [2.824(2)−2.891(2) Å].[4] The Rh−Ge distances to the two terminally

(17) Manson, J.; Webster, C. E.; Hall, M. B. *JIMP*, development version 0.1.v117 (built for Windows PC and Redhat Linux); Department of Chemistry, Texas A&M University: College Station, TX. http://www.chem.tamu.edu/jimp/ (accessed July 2004).

(18) *MOPLOT2 for orbital and density plots from linear combinations of Slater or Gaussian type orbitals*, version 2.0; Lichtenberger, D. L., Ed.; Department of Chemistry, University of Arizona: Tucson, AZ, 1993.

(19) Tomotake, Y; Matsuzaki, K.; Murayama, K.; Watanabe, E.; Wada, K.; Onoda, T. *J. Organomet. Chem.* **1987**, *320*, 239–247.

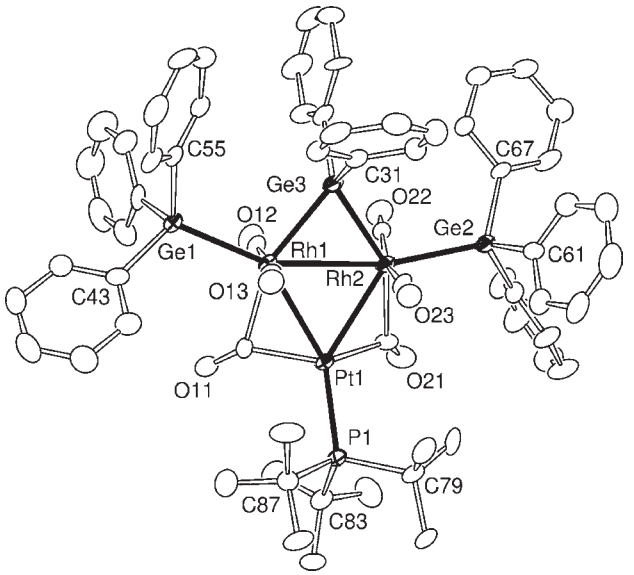

Figure 3. An ORTEP diagram of the molecular structure of $PtRh_2(CO)_6(GePh_3)_2(PBu^t_3)(\mu\text{-}GePh_2)$, **5**, showing 30% thermal ellipsoid probability. Selected bond distances (Å) and angles (deg) are as follows: Rh(1)−Rh(2) = 2.9295(12), Rh(1)−Ge(1) = 2.5035(13), Rh(2)−Ge(2) = 2.5085(14), Rh(1)−Ge(3) = 2.4865(14), Rh(2)−Ge(3) = 2.4866(13), Rh(1)−Pt(1) = 2.7647(9), Pt(1)−Rh(2) = 2.7897(9); Rh(1)−Ge(3)−Rh(2) = 72.18(4), Rh(1)−Rh(2)−Ge(3) = 53.91(3), Rh(2)−Rh(1)−Ge(1) = 157.86(5), Rh(1)−Pt(1)−Rh(2) = 63.66(3), Rh(1)−Rh(2)−Pt(1) = 57.76(2).

coordinated $GePh_3$ ligands, 2.4961(7) and 2.5000(7) Å [2.5059(6) and 2.4821(7) Å for molecule **2**] are similar to the 2.5061(4) Å Rh−Ge distance found in **3** and the 2.480(3) Å distance found in **1**.[12] The Rh−Ge distances to the bridging $GePh_2$ ligand, Rh(1)−Ge(3) = 2.4728(6) and Rh(2)−Ge(3) = 2.4815(7) Å and Rh(3)−Ge(6) = 2.4706(6) Å, Rh(4)−Ge(5) = 2.4821(7) Å, and Rh(4)−Ge(6) = 2.4847(7) Å for molecule **2**, are similar to the Rh−Ge distances to the bridging $GePh_2$ ligands in **1**, range 2.461(3)−2.522(3) Å.[12]

In previous studies, it was found that $Pt(PBu^t_3)$ groups generated from the compound $Pt(PBu^t_3)_2$ can be added across Ru−Ru bonds,[20] Os−Os bonds,[21] Ir−Ir bonds,[22] Rh−Rh bonds,[23] Re−Sn bonds,[24] and Re−Ge bonds[24] to form larger clusters in which the platinum atom is bonded to both the transition metals and the main group metal atoms. As expected when **4** is allowed to react with $Pt(PBu^t_3)_2$, a $Pt(PBu^t_3)$ adduct of **4**, $PtRh_2(CO)_6(\mu\text{-}GePh_2)(GePh_3)_2(PBu^t_3)$, **5**, was formed in 42% yield. This orange compound is the only one in this series that is stable in the absence of CO, but it does slowly decompose in air over a period of a few days. Compound **5** was characterized by IR, ^{1}H and ^{31}P NMR, and a single crystal X-ray diffraction analysis. An ORTEP diagram of the molecular structure of **5** is shown in Figure 3. Both rhodium atoms have a pentagonal bipyramidal structure. The two rhodium atoms are mutually-bonded, Rh(1)−Rh(2) = 2.9295(12) Å. This distance is only slightly longer than the Rh−Rh distance in **4**. Each rhodium atom is bonded to the platinum atom, a terminal $GePh_3$, a bridging $GePh_2$, two terminal CO ligands, and one bridging CO across the Rh−Pt bonds. The Rh−Ge distances of 2.5035(13) and 2.5085(14) Å to the terminal $GePh_3$ ligands are similar to those in **3** (2.5061(4) Å) and **4**. The Rh−Ge distances to the bridging $GePh_2$ ligand, 2.4865(14) Å and 2.4866(13) Å, are also similar to those in **4**, see above. Two of the CO ligands, one from each rhodium atom, have formed bridges to the platinum atom, Pt(1)−C(11) = 1.990(11) Å, Pt(1)−C(21) = 2.002(12) Å, Rh(1)−C(11) = 2.169(12) Å, Rh(2)−C(21) = 2.142(11) Å. The platinum atom exhibits strong one bond coupling to the phosphorus atom of the phosphine ligand in the ^{31}P NMR spectrum, δ = 107.16, $^1J_{^{195}Pt-^{31}P}$ = 4993 Hz. The equivalent rhodium atoms exhibit small two bond coupling to the phosphorus atom, $^2J_{^{103}Rh-^{31}P}$ = 8.1 Hz.

Simple electron counting procedures suggest that compounds **4** and **5** should contain a rhodium−rhodium bond so that these metal atoms can achieve 18 electron configurations. In order to understand the bonding in **4** and **5**, Fenske−Hall (FH) molecular orbital analyses were performed. To simplify the calculations, the phenyl groups on the $GePh_3$ and $GePh_2$ ligands and the t-butyl groups on the phosphine ligands were replaced by hydrogen atoms to give GeH_3, GeH_2, and PH_3, respectively. The molecular symmetry of **4** is approximately C_{2v}. Diagrams of the lowest unoccupied molecular orbital (LUMO) and some selected occupied molecular orbitals of **4** are shown in Figure 4. As expected, the LUMO, Figure 4a, in **4** is a σ-antibonding orbital associated with the Rh−Rh bond. The highest occupied molecular orbital (HOMO) at −7.78 eV is predominantly the Rh−Rh bond, Figure 4b. The bonding between the rhodium atoms and the bridging GeH_2 ligand is shown by the antisymmetric HOMO−1 at −9.61 eV and the symmetric HOMO−2 at −9.68 eV, Figure 4c and d. The symmetric HOMO−9 at −13.24 eV, Figure 4e, shows bonding between the two rhodium atoms that includes significant interactions with the terminal GeH_3 ligands.

Selected Fenske−Hall molecular orbitals of **5** are shown in Figure 5. In these orbitals, one can see how the addition of the platinum atom affects the orbitals in **5**. The LUMO (Figure 5a) is still Rh−Rh antibonding. The HOMO (Figure 5b) at −7.78 eV shows that the Rh−Rh bonding is delocalized and significantly involves the platinum atom. The importance of delocalization in the bonding of $Pt(PBu^t_3)$ groups to metal−metal bonds has been found in a number of related systems.[20,22] The HOMO−1 and HOMO−2, Figure 5c and d, respectively, correspond to the HOMO−2 and HOMO−1 in **4**. The reversal in order indicates that the platinum atom in **5** interacts more strongly with the HOMO−1 in **4** than it does with the HOMO−2. The formation of the bonding interactions between the platinum atom and the two bridging CO ligands contributes significantly to the stabilization of the unsymmetric HOMO−2 orbital in **5**. The HOMO−14 at −13.16 eV is shown in Figure 5d. It is derived from the interactions of the platinum atom with the HOMO−9 of **4** and represents another component of the strong delocalized bonding between the platinum atom and two rhodium atoms.

(20) (a) Adams, R. D.; Trufan, E. *Organometallics* **2008**, *27*, 4108–4115. (b) Adams, R. D.; Captain, B.; Fu, W.; Hall, M. B.; Smith, M. D.; Webster, C. E. *Inorg. Chem.* **2004**, *43*, 3921–3929.
(21) Adams, R. D.; Captain, B.; Zhu, L. *Inorg. Chem.* **2007**, *46*, 4605–4611.
(22) Adams, R. D.; Captain, B.; Hall, M. B.; Smith, J. L., Jr.; Webster, C. E. *J. Am. Chem. Soc.* **2005**, *127*, 1007–1014.
(23) Adams, R. D.; Captain, B.; Pellechia, P. J.; Smith, J. L., Jr. *Inorg. Chem.* **2004**, *43*, 2695–2702.
(24) Adams, R. D.; Captain, B.; Herber, R. H.; Johansson, M.; Nowik, I.; Smith, J. L., Jr.; Smith, M. D. *Inorg. Chem.* **2007**, *46*, 4605–4611.

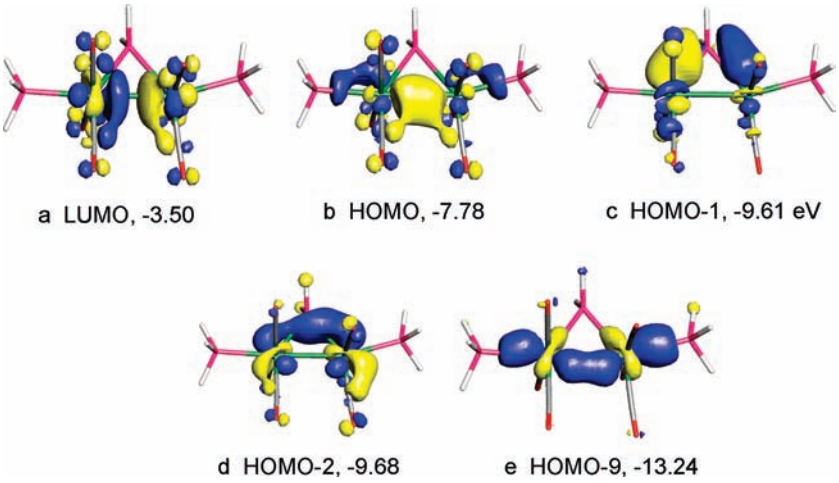

Figure 4. Selected Fenske−Hall molecular orbital diagrams for **4** showing the Rh−Rh and Rh−Ge bonding.

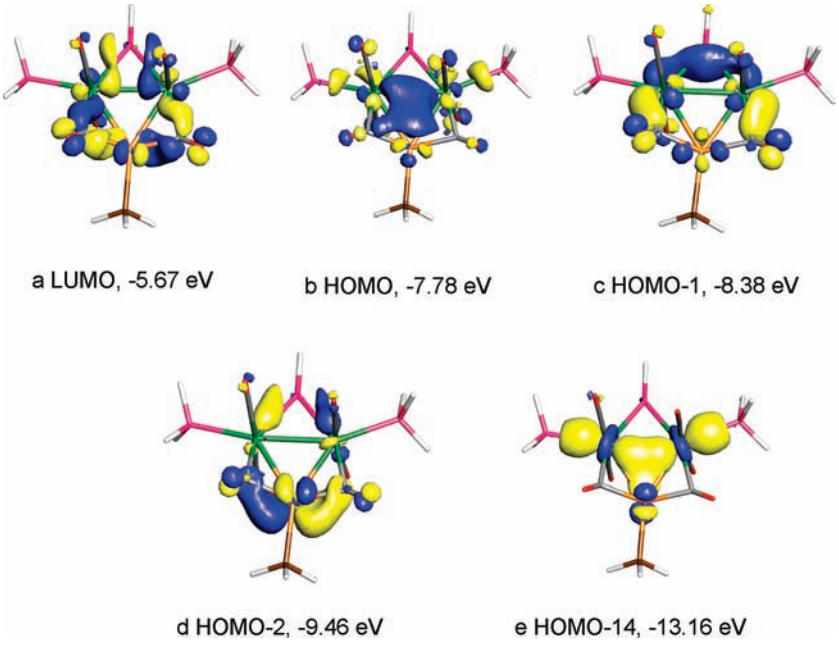

Figure 5. Selected Fenske−Hall molecular orbital diagrams for **5** showing the Rh−Rh, Rh−Pt, and Rh−Ge bonding.

Scheme 1

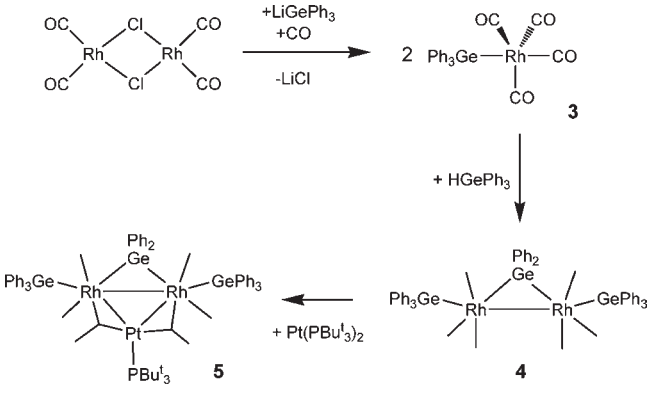

Summary

A summary of the reactions described in this report is shown in Scheme 1. The new rhodium−germanium complex **3**, obtained from the reaction of Ph_3GeLi with $[Rh(CO)_2Cl]_2$ in the presence of a CO atmosphere, is the first structurally characterized rhodium complex with the general formula $RRh(CO)_4$. The dirhodium reagent $[Rh(CO)_2Cl]_2$ was split in two when the bridging chloro ligands were replaced by the terminally coordinated $GePh_3$ ligand. The rhodium atoms add two more CO ligands to form an 18 electron complex which is stable only under a CO atmosphere. Even removal of the solvent and CO from the reaction mixture *in vacuo* resulted in complete decomposition of the complex. Compound **3** was found to react with $HGePh_3$ to yield the dirhodium complex **4**. The formation of **4** clearly involved two equivalents of **3**, a loss of a CO ligand from each of the two molecules of **3**, formation of a Rh−Rh bond, and the formation of a bridging $GePh_2$ ligand across the newly formed Rh−Rh bond. The $GePh_2$ group evidently formed by cleavage of a phenyl group from a $GePh_3$ group which then combined with the hydrogen atom of the $HGePh_3$ reagent to form benzene.[25] Compound **4** is more

(25) Adams, R. D.; Captain, B.; Trufan, E. *J. Cluster Sci.* **2007**, *18*, 642–659.

stable than **3**, but it still decomposes readily in the absence of a CO atmosphere. The reaction of **4** with $Pt(PBu^t_3)_2$ yielded the new trinuclear metal complex **5** by the loss of one PBu^t_3 ligand from the $Pt(PBu^t_3)_2$ and the addition of the resultant $Pt(PBu^t_3)$ group across the Rh−Rh bond of **4**. We have now observed a large number of such addition reactions involving both the $Pt(PBu^t_3)$ group[20,21] and the $Pd(PBu^t_3)$ group.[26−29]

(26) Adams, R. D.; Captain, B.; Smith, M. D. *J. Cluster Sci.* **2004**, *15*, 139–149.
(27) Adams, R. D.; Captain, B.; Fu, W.; Hall, M. B.; Manson, J.; Smith, M. D.; Webster, C. E. *J. Am. Chem .Soc.* **2004**, *126*, 5253–5267.
(28) Adams, R. D.; Captain, B.; Boswell, E. *Organometallics* **2008**, *27*, 1169–1173.
(29) Adams, R. D.; Captain, B. *Acc. Chem. Res.* **2009**, *42*, 409–418.

Acknowledgment. This research was supported by the National Science Foundation under Grant No. CHE-0743190. We thank the USC NanoCenter for partial support of this work.

Supporting Information Available: CIF tables for the structural analyses of **3**−**5**. This material is available free of charge via the Internet at http://pubs.acs.org.